Available online at www.sciencedirect.com
ScienceDirect
Journal of the European Ceramic Society 29 (2009) 1647–1656
www.elsevier.com/locate/jeurceramsoc

Degradation of plasma-sprayed yttria-stabilized zirconia coatings via ingress of vanadium oxide☆

Zun Chen [c], Jim Mabon [b], Jian-Guo Wen [b], Rodney Trice [a,*]

[a] School of Materials Engineering, Purdue University, West Lafayette, IN 47907, United States
[b] Frederick Seitz Materials Research Laboratory, University of Illinois at Urbana-Champaign, Urbana, IL 61801, United States
[c] McCormick School of Engineering, Northwestern University, Evanston, IL 60208, United States

Received 11 July 2008; received in revised form 23 September 2008; accepted 2 October 2008
Available online 13 November 2008

Abstract

V_2O_5 reaction and melt infiltration in plasma-sprayed 7 wt% Y_2O_3–ZrO_2 (YSZ) coatings were investigated at temperatures ranging from 750 °C to 1200 °C using SEM and TEM combined with EDS. The interlamellar pores and intralamellar cracks, common in plasma-sprayed materials, provide pathway for the molten species. The microstructure of the contaminated coatings is therefore the result of the interplay between the dissolution/reaction rates of the V_2O_5 with YSZ coating and the infiltration rates of the molten species. Near the coating surface, the reaction front proceeds in a planar fashion, via dissolution of the lamella and precipitation of fine-grained reaction products composed of ZrV_2O_7 (for reactions at 750 °C and below), m-ZrO_2 and YVO_4. The thickness of this planar reaction zone or PRZ was found to increase as reaction time and temperature increased. The melted V_2O_5 was observed to infiltrate along the characteristic microstructure of plasma-sprayed coatings, i.e. the interconnected pores and cracks, and react with the YSZ. The thickness of this melt infiltrated reaction zone or MIRZ ranged from 5 μm for reactions at 750 °C for 30 min to 130 μm for reactions at 1000 °C for 90 min. At 1200 °C, only a PRZ was observed (i.e. the thickness of the MIRZ was nominally zero), suggesting that the dissolution reaction within the pores/cracks and subsequent formation of reaction products may limit infiltration. Fifty-hour heat-treatments at 1000 °C and 1200 °C prior to reaction with the V_2O_5 at 800 °C for 90 min were used to change the microstructural features of the coating, such as crack connectivity and pore size. The heat-treatment at 1000 °C was found most deleterious to the coating due to large cracks created via a desintering process that afforded deep penetration of the molten V_2O_5.

Keywords: ZrO_2; Corrosion; V_2O_5; Infiltration; Plasma-sprayed coating

1. Introduction

Thermal barrier coating (TBC) systems are used as protective layers in gas turbine engines. In conjunction with component cooling, TBC systems reduce the surface temperature of the underlying structural component, making it possible to increase the operating temperature of the turbine, and therefore its efficiency.[1] A well-engineered TBC system can withstand the severe combustion environment for long enough time to justify their application, providing sufficient thermal insulation and prevention of substrate oxidation.[2] Despite the effectiveness of the coatings, the use of TBCs in turbines using syngas is limited. The main concern has been the deleterious effect of the elevated amounts of Fe, Ni, S, N, As and V impurities in the syngas[3] on TBCs. The impurities in the highly contaminated fuel can combine to form molten salts, such as sodium sulfate and vanadium compounds in the combustion environment, giving rise to hot corrosion problems. Hot corrosion degrades the yttria-stabilized zirconia (YSZ) top coat at higher rate than that in the absence of molten salts. In fact, failure of the top coat caused by molten salt can precede failures due to sintering, the development of a thermally grown oxide, and the phase change of the as-sprayed YSZ, which only become significant after more than thousands of hours in service.[4] In contrast, cracking or delamination of

☆ This work was supported by Purdue Research Foundation and by the National Science Foundation through DMR-0134286. STEM, SEM and EDS analysis in this work was carried out in the Center for Microanalysis of Materials, University of Illinois, which is partially supported by the U.S. Department of Energy under grant DEFG02-91-ER45439.
* Corresponding author.
E-mail address: rtrice@purdue.edu (R. Trice).

0955-2219/$ – see front matter © 2008 Elsevier Ltd. All rights reserved.
doi:10.1016/j.jeurceramsoc.2008.10.003

the top coat was found to occur within 1000 h or 500 1-h cycles during hot corrosion tests when TBC systems were exposed to various of molten salts.[5,6]

The degradation of YSZ coatings via reaction and infiltration of molten salts can be chemical or mechanical in nature. For example, substantial chemical attack occurs when vanadium-containing melts contact YSZ. This attack can remove the affected layer of the coating, or simply replace the original tetragonal zirconia phase with the less desirable reaction products[7,8] like YVO_4 and a m-ZrO_2.[9] Even if the infiltrant does not react extensively with the coating, its presence in the near-surface layer can cause failure in the coating. For example, Kramer et al.[10] studied the interaction of environmental deposits of calcium-magnesium-alumina-silicate (CMAS) with electron beam physical vapor deposited thermal barrier coatings. Their results showed that although the infiltration of the melt took place rapidly, the attack was minimal in the bulk of the coating. But, Mercer et al.[11] showed that CMAS infiltration into the coating can make the affected layer have a substantially different compliance compared to the un-infiltrated part of the coating. This makes the infiltrated layer more susceptible to exfoliation upon cooling. An additional failure mechanism of the top coat is delamination caused by reaction of molten salts with the chemically more vulnerable bond coat after complete infiltration through the top coat.[12] As molten salts are usually found to penetrate through the thickness of the top coat in hot-corroded coatings,[13] all three mechanisms contribute to the failure of the coatings. The extent of the reaction and ingression of the melt, and hence the dominant failure mechanism, however, is determined by the composition of the molten salts. Of interest in this work is vanadium oxide, which will both dissolve and react, and infiltrate and react with plasma-sprayed YSZ coatings.

Vanadium pentoxide (V_2O_5) is a combustion product of petroleum crude and fuel oils.[14] With a melting temperature of 690 °C, molten V_2O_5 has a substantial vapor pressure, e.g., 5 Pa at 827 °C and 52 Pa at 1027 °C.[15] V_2O_5 may also combine with Na_2O to form $NaVO_3$ or Na_3VO_4.[16] A study on the reaction of V_2O_5 with dense single crystal and polycrystalline cubic YSZ showed that a eutectic solution formation along with the phase separation led to a highly corroded surface.[17] In an accompanying paper,[18] the reaction mechanism between V_2O_5 and plasma-sprayed YSZ will be presented. In summary, the phase evolution that occurs between V_2O_5 and a plasma-sprayed yttria-stabilized zirconia coating from 700 to 900 °C was investigated *in situ* by X-ray diffraction. Concurrent formation of ZrV_2O_7 and YVO_4 were observed at 700 °C and 750 °C, suggesting a similar reactivity of yttria and zirconia with vanadium oxide. The ZrV_2O_7 partially decomposed into m-ZrO_2 subsequently after 150 and 60 min at 700° and 750 °C, respectively. For reaction temperatures of 800 and 900 °C, the reaction products were m-ZrO_2 and YVO_4. The dissolution of both Y_2O_3 and ZrO_2, the rate of which increases dramatically with temperature, is largely responsible for the degradation of the coating. Ultimately, the reaction between the molten V_2O_5 and the YSZ turned the lamellar structure near the surface of the coating into fine equiaxed particles.

Pore morphology in plasma-sprayed coatings plays a vital role on melt infiltration. The as-sprayed YSZ coating is a built-up of lamellae composed of columnar grains, with numerous pores and cracks in between.[19,20] Most commonly seen are intralamellar cracks oriented along the boundaries of columnar grains, and interlamellar pores between lamella. Interlamellar pores are oriented parallel to the coating surface. These pores are ~0.1 μm in at least one dimension. The interlamellar pores and intralamellar cracks can form an interconnected network throughout the coating, affording deep penetration of liquids into the YSZ.

Regarding the infiltration of vanadium-containing molten salt in porous YSZ coatings, Park et al.[21] recently studied the ingress of a corrosive melt, $NaVO_3$, in plasma-sprayed YSZ coatings. Their study revealed the important role of pores, microcracks and lamella boundaries on the ingression and degradation of the coatings. They demonstrated that a coating with 4% porosity retarded the monoclinic transformation as compared to its counterpart with 9% porosity. Compared to $NaVO_3$, V_2O_5 is expected to more aggressively attack the YSZ coating. Thus, an investigation of the dissolution/reaction and infiltration of a highly aggressive molten oxide will provide insight into the competing dissolution, reaction and infiltration processes.

This paper addresses the interplay between the dissolution, reaction, and infiltration rates of molten V_2O_5 into porous plasma-sprayed YSZ coatings. Surface reaction and infiltrated regions were identified using SEM and TEM, which were complemented by concentration profiles constructed from EDS measurements. Dissolution, reaction, and infiltration rates of the V_2O_5 with the YSZ were varied by adjusting the temperature of the oxide melt (750–1200 °C), reaction time (30–420 min) and via heat-treatments of 50-h at 1000 °C or 1200 °C of the YSZ coating prior to the hot-corrosion experiment. These heat-treatments were expected to change and/or densify the coating microstructure, thus affecting the infiltration path.

2. Experimental procedures

2.1. Coating preparation

A 7 wt% Y_2O_3–ZrO_2 (YSZ) powder with an average particle size of 22 μm (H.C. Starck, Amperit 825.0) was air-plasma sprayed using a Praxair SG-100 gun at Ames National Laboratory using conventional spray parameters, including a gun power of 38 kW. Flat copper plate substrates of 102 mm × 76 mm × 5 mm were grit blasted with 24-grit Al_2O_3 at 5.5×10^5 Pa prior to being sprayed. The substrates were back-cooled with air jets while sprayed from a stand-off distance of ~10 cm. Stand-alone coatings were obtained by dissolving the Cu substrates with nitric acid. The resultant coating thickness varied from 360 to 590 μm. Archimedes experiments[22] in water indicated a total porosity of 10.8% based on a theoretical density of 6.08 g/cm^3. This porosity was in the form of intralamellar microcracks and interlamellar pores. The coatings were subsequently sectioned into 1 cm × 1 cm squares with a diamond-coated saw for corrosion tests.

2.2. Corrosion procedures

Approximately 10 mg/cm^2 V_2O_5[1], or 3 wt% of the weight of the coating sample, was sprayed on the surface of the stand-alone coatings using an air brush. The V_2O_5 powder was ballmilled with ethanol to facilitate spraying. The V_2O_5/coating was then placed in an alumina crucible which was subsequently covered with a thin alumina sheet during heat-treatment. The assembly was placed in a box furnace which was preheated to the target temperature. The temperature of the furnace was restored within 5 min of opening and closing its door to insert the sample. Note that experiments conducted at 1100 °C and below used this furnace. For tests performed at 1200 °C, the assembly was placed in the furnace at 25 °C and then heated at a rate of 600 °C/h.

Hot corrosion tests involving molten vanadium oxide were carried out for 30, 70, 180 and 420 min at 750 °C, as well as for 30, 60, 150 min at 800 °C on stand-alone as-sprayed YSZ coatings. According to *in situ* XRD results,[18] these time periods are when significant reaction between V_2O_5 and YSZ takes place at 750 °C and 800 °C.[18] Additional tests were performed at 900°, 1000° and 1200 °C for 90 min to investigate the effects of higher reaction temperatures on the reaction and infiltration of the coating. Hot corrosion experiments (800 °C for 90 min) were also performed on coatings that had been previously heat-treated for 50-h at 1000 °C and 1200 °C, simulating the in-service coating microstructures.

2.3. Microscopy procedures

The reacted coatings were mounted in the cross-sectional orientation, polished, and examined with a JEOL JSM-7000F Field Emission Analytical SEM equipped with an energy dispersive spectroscopy (EDS) unit that used stored or fitted standards. The SEM was operated with a 30 keV accelerating voltage, which was high enough to generate the K_α lines of Zr, Y, and V. Beginning at the top of the coating, EDS point scans were taken at an interval of 3–10 μm through the thickness direction to measure the ingression of V and the distribution of Y and Zr atoms. The interval depended on the overall reaction depth into the coating, with larger intervals chosen for greater reaction depths. Concentration profiles of the coating were constructed by plotting the mole percent of Zr, Y, and V versus the thickness of the coating. The concentration of atomic species reported is an average value because the probe size of the e-beam (∼1 μm) was larger than the pores and cracks in the coating. However, the concentration profile through the coating thickness provides a trend for vanadium oxide ingression.

Scanning transmission electron microscope (STEM) specimens were made from coatings reacted with ∼3 wt% V_2O_5 for 3 h at 750 °C. Cross-sectionally oriented specimens were prepared by first gluing two piece of coating together with the reacted zones (i.e. the top of the coatings) back to back. A wedge-shaped coating was prepared by adjusting the tilting angle of a tripod polisher. The specimen was polished progressively on both sides using a sequence of diamond-coated polishing films coated (30, 5 and 1 μm) until the thin end of the wedge began to recede. The specimen was subsequently mounted on a nickel grid and further thinning was performed using a low-energy Gatan ion mill, model DMP 600. The specimens were investigated in a JEOL 2010F (S)TEM capable of EDS mapping. Both the SEM and STEM used in this study were located at the Center for Microanalysis of Materials at the University of Illinois.

3. Results

3.1. Overview of reacted microstructure

As illustrated in the schematic in Fig. 1(a), reacted coatings generally displayed a reaction zone comprised of two regions, each with a different morphology. The planar reaction zone (PRZ) and melt infiltrated reaction zone (MIRZ) were observed in a reacted coating only when there was significant dissolution and reaction between the top of the coating and the molten V_2O_5, and sufficient infiltration rates of the V_2O_5 into the coating prior to closure of the cracks and pores by the reaction products. The PRZ proceeds in a more-or-less planar fashion as shown in Fig. 1(a). Fig. 1(b) shows that the microstructure of the PRZ is composed of equiaxed grains and EDS results indicated (not shown) this region to have a vanadium concentration equal or greater than the Y concentration. The interaction in the PRZ is primarily a dissolution–precipitation type reaction where the YSZ coating is dissolved in molten vanadium oxide and precipitates as yttrium vanadate and either zirconia vanadate or monoclinic zirconia depending on the test temperature and time of reaction.[18] Note that original lamellar structure is no longer distinguishable in the PRZ.

The MIRZ, shown in Fig. 1(c), appears as a dense microstructure but the lamellar structure is largely preserved. Molten vanadium oxide in the MIRZ is transported via melt infiltration and no vanadium is detected using EDS beyond the MIRZ. A fractured cross section of an unaffected region is shown in Fig. 1(d). Note the lamellar microstructure, as well as the presence of porosity between the unaffected lamella. Cracks oriented perpendicular to the lamella are not evident in the micrograph presented in Fig. 1(d), but were evident in other SEM micrographs of the coating surfaces not presented in the current work. Thus, the unaffected regions can be considered to have the typical microstructure associated with a plasma-sprayed coating, i.e. residual porosity and microcracks.

3.2. Development of the PRZ and MIRZ as a function of time at 750 and 800 °C

Fig. 2 shows the cross-sectional view of a YSZ coating after a 30-min reaction with V_2O_5 at 750 °C. The sample was fractured at room temperature following the reaction and viewed in a SEM. Note the unreacted, but clearly melted, V_2O_5 fused phase on the surface of coating. The thickness of this layer was 2–5 μm. An EDS point scan at point 1 (i.e. within the fused phase) indicated this region to be 26.9 mol.% V, with less than 2 mol.% Y and Zr combined (balance of O). Beyond the fused

[1] Alfa Aesar (Ward Hill, MA), catalog # 11094, powder form.

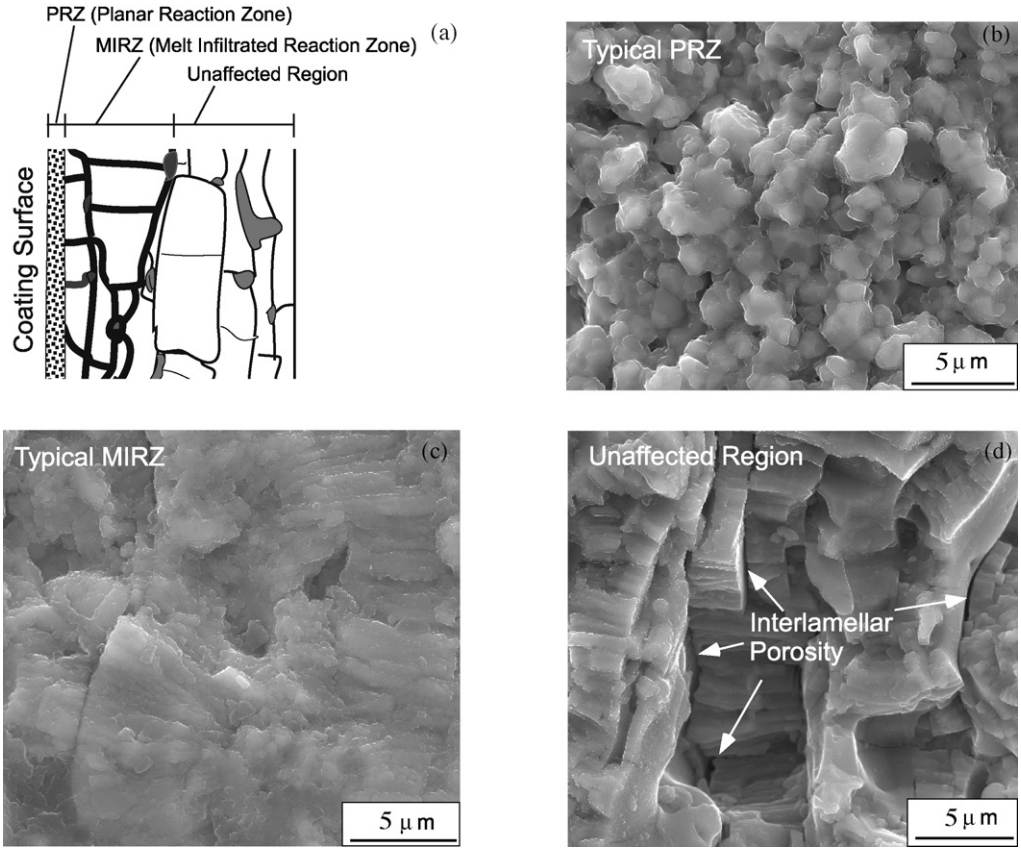

Fig. 1. (a) Schematic illustrates two distinct regions through the thickness of a plasma-sprayed coating reacted with V_2O_5 above its melting temperature. The two regions observed were a planar reaction zone (PRZ) and a melt infiltrated reaction zone (MIRZ). The SEM micrographs that follow show the characteristic morphologies that are found in each respective region. These micrographs are taken from fractured surfaces perpendicular to the coating surface. Image (b) depicts clusters of equiaxed particles, typical of PRZ, after the coating reacted with vanadium oxide for 3 h at 1200 °C. Image (c) depicts lamellar structure that is preserved to some extent in MIRZ. The sample had reacted with V_2O_5 at 750 °C for 420 min. Image (d) shows the intact lamellar structure when unaffected by V_2O_5 penetration.

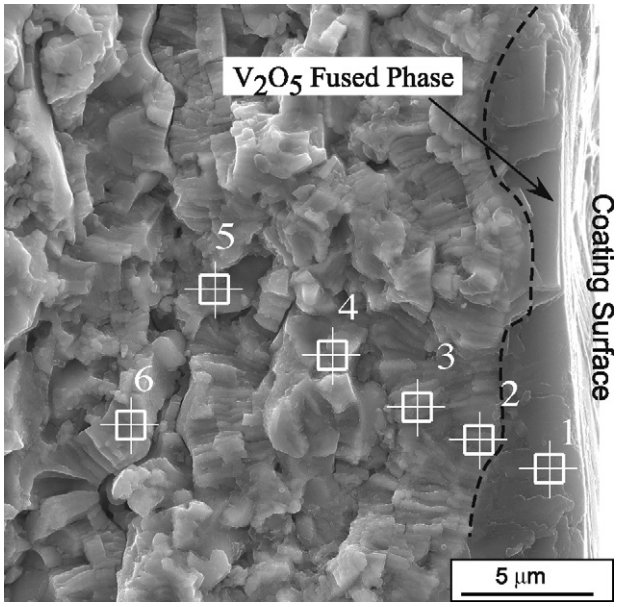

Fig. 2. Fractured cross section surface after YSZ coating reacted with 3 wt% V_2O_5 for 30 min at 750 °C.

phase, the characteristic lamellar microstructure was still evident with no equiaxed microstructure characteristic of the PRZ noted. However, EDS results confirmed that infiltration of the molten V_2O_5 has already occurred. Point 2 on Fig. 2 indicated a V content of 2.4 mol.%, but this diminished to zero at point 3 on the micrograph. Thus, there was limited infiltration of V_2O_5 with the YSZ after 30 min at 750 °C.

To study the time-dependent interaction kinetics at 750 °C, the reaction between V_2O_5 and YSZ was interrupted after 70 min, 180 min and 420 min. Fig. 3(a)–(c) shows the backscattered electron SEM micrographs of the polished cross section of the coatings. No visible PRZ was observed in the coating after 70 min. EDS results (not shown) indicated the presence of vanadium at a depth of approximately 50 μm below the surface. EDS results, combined with the observation of the coating as shown in Fig. 3(a), establishes an MIRZ of 50 μm after 70 min at 750 °C. With increasing time at 750 °C, the thickness of the PRZ increases from nominally zero after 70 min to ~15–20 μm and ~30–40 μm after 180 and 420 min, respectively. These thickness values were determined from the micrographs in Fig. 3(b and c), and are indicated by the black dotted lines. The thickness of the MIRZ layer was ~5 μm after 30 min, and constant at ~50 μm for all times investigated. The overall penetration depth (i.e. the PRZ thickness plus the MIRZ thickness) was ~5, ~50,

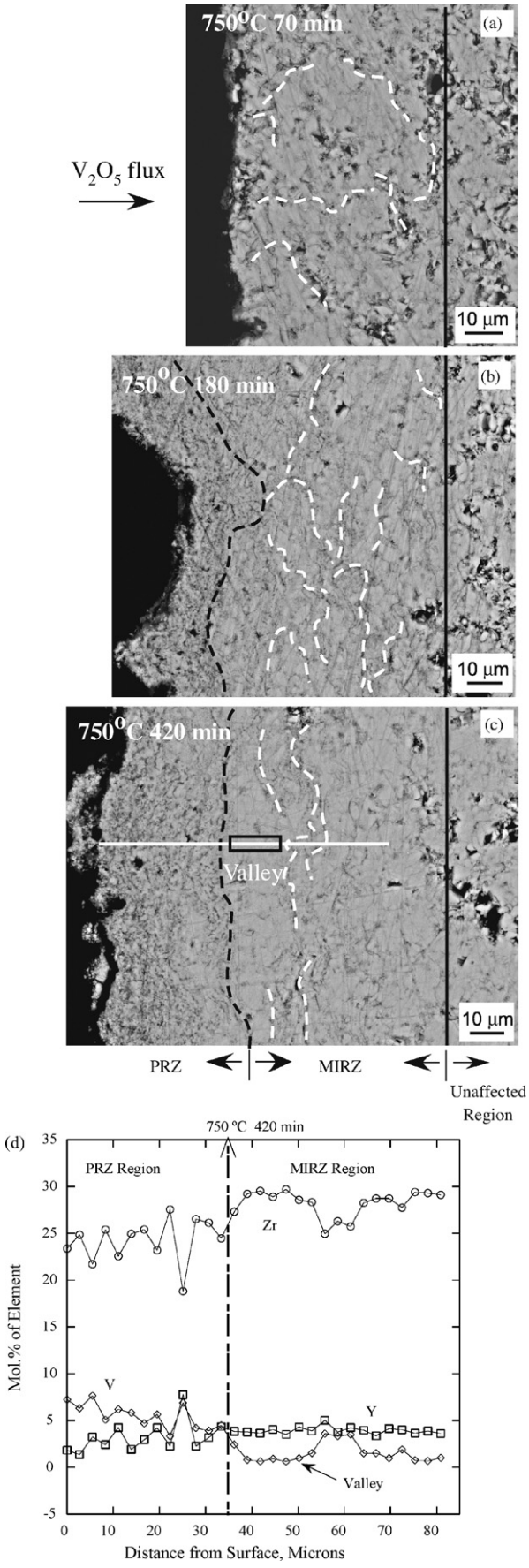

Fig. 3. Backscattering SEM micrographs of coating cross sections after reacting with 3 wt% V_2O_5 for (a) 70 min, (b) 180 min and (c) 420 min at 750 °C. Image (d) is the concentration profile after 420 min at 750 °C along the horizontal white line indicated in image (c). The balance is oxygen.

~60–70, and ~80–90 μm at 750 °C for reaction times of 30, 70, 180, and 420 min, respectively.

Fig. 3(d) is the molar concentration profile of Zr, Y and V for the coating reacted with V_2O_5 at 750 °C for 420 min. The PRZ thickness determined from the microscopy investigation (see Fig. 3(c)) coincides with the distance from the coating surface where the V concentration is higher than or approximately equal to the Y concentration. Since the final reaction product, YVO_4, has a V:Y atomic ratio of 1:1, it is reasonable that the concentrations of Y and V are comparable in this region.

Within the MIRZ region indicated in Fig. 3(d), the V concentration profile typically exhibits a "zig-zag" profile where the V concentration varies from 0 to 1–3 mol.%. The local peaks in V concentration were linked to large interconnected porosity in the coating that was filled by the infiltrating vanadium oxide. These regions are highlighted in Fig. 3(c) with white dashed lines. Note that in comparison to the unaffected regions, where large amounts of porosity are observed between lamella, that the MIRZ regions appear dense.

The effect of time on the reaction and infiltration kinetics at 800 °C was also studied, interrupting the reaction between the V_2O_5 and YSZ after 30, 60 or 150 min. The reacted coatings displayed no PRZ for either the 30 or 60 min heat-treatments at 800 °C. Based on microscopy measurements coupled with concentration profiles for each reaction time at 800 °C (not shown), the penetration depth of samples tested at 800 °C for 30, 60 and 150 min were equal at ~80 μm. Because the penetration depth was approximately constant with infiltration time, an upper bound for melt infiltration of 30 min at 800 °C can be established.

It is important to point out that while the MIRZ forms via infiltration of the interconnected pores and cracks, the reaction that occurs between the vanadium oxide and the YSZ within the pores and cracks would be expected to be the same reaction that leads to the development of the PRZ. Thus, the same dissolution and precipitation reaction that forms the equiaxed microstructure observed in the PRZ (see Fig. 1(b)) also occurs in the infiltrated pores. An example of this is noted in Fig. 4, which shows the filling of a pore by the equiaxed reaction product. There is an 8–9% increase in the molar volume associated with the reaction of V_2O_5 and YSZ to form YVO_4 and m-ZrO_2. For reaction of V_2O_5 with plasma-sprayed YSZ at 750 and 800 °C, it is clear that infiltration of the molten liquid occurs more rapidly than the formation of reaction products. In other words, there is sufficient time for infiltration prior to the reaction products filling the cracks and pores and a MIRZ under these conditions.

3.3. Effect of 900°, 1000°, and 1200 °C reaction temperatures on the formation of the PRZ and MIRZ

The microstructures formed when V_2O_5 reacts with YSZ after 90 min at 900, 1000, and 1200 °C are shown in Fig. 5.

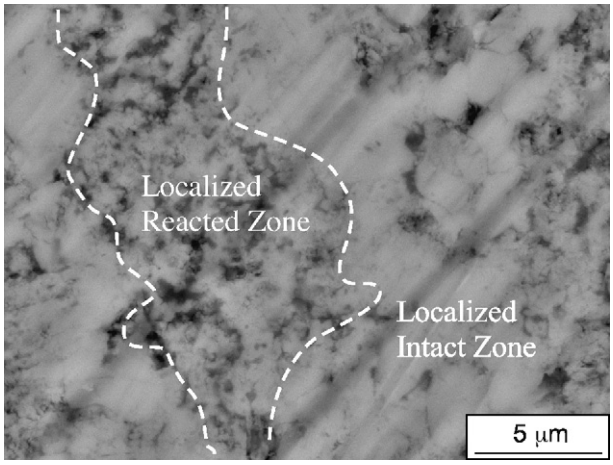

Fig. 4. Backscattered SEM micrographs showing the localized fine-grained reacted zone in a coating reacted with vanadium oxide for 60 min at 800 °C. The white dashed lines highlight the reaction zone in the MIRZ.

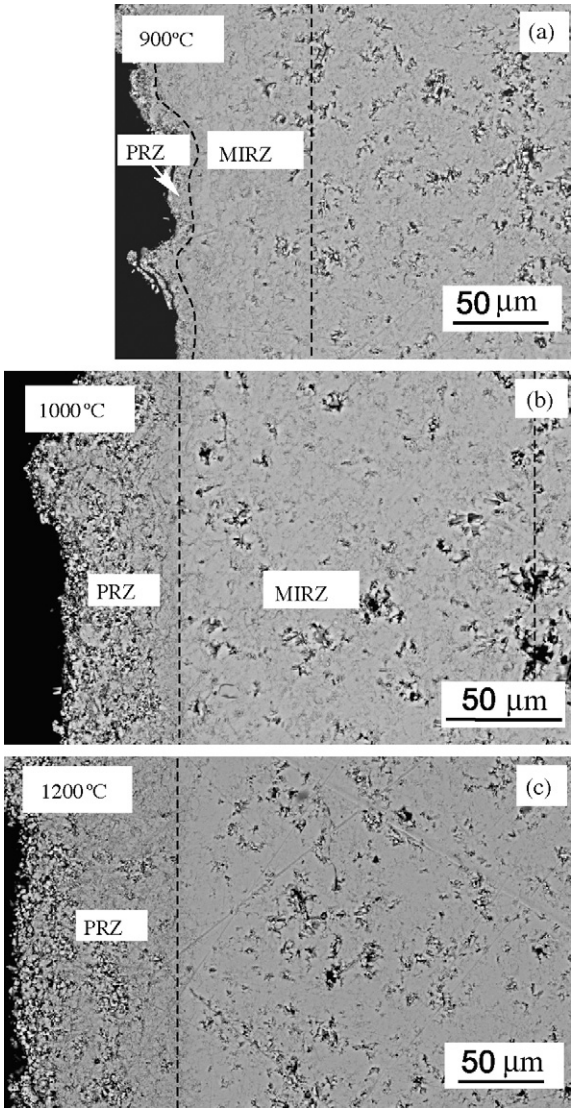

Fig. 5. Backscattered SEM micrographs of coating cross sections after reacting with V_2O_5 for 90 min at (a) 900 °C, (b) 1000 °C and (c) 1200 °C, with PRZ and MIRZ regions noted.

The thickness of the PRZ increases as the reaction temperature increases, with a thickness of ~10, ~50 and ~100 μm measured at 900, 1000 and 1200 °C, respectively.

The thickness of the MIRZ was 50 μm, 130 μm, and 0 μm after 90 min at 900, 1000, and 1200 °C, respectively. In the MIRZ region there existed the "zig-zag" concentration profile noted previously where the V concentration varied from 0 to 1–3 mol.% as a function of depth into the coating; this is consistent with infiltration of the molten V_2O_5 into the coating. However, there was no detectable vanadium beyond the PRZ for experiments at 1200 °C. The porous PRZ top layer formed at reaction temperatures of 1000 °C and 1200 °C was loosely bonded to adjacent particles and would likely be susceptible to erosion.

3.4. Microstructural observation of infiltrated pores and cracks

Evidence of the infiltration of the vanadium-containing melt through the porous features common in plasma-sprayed coating is shown in Fig. 6(a) and (b), which are STEM micrographs in the MIRZ after a 180-min reaction with vanadium oxide at 750 °C. In Fig. 6(a), the image contrast reveals a compositionally distinct region along an interlamellar pore. The darker contrast phase contains a high vanadium content while the lighter contrast surrounding phase is composed of Zr, Y and O, with no vanadium detected. Among the possible transport mechanisms of vanadium oxide, namely, reaction, diffusion and infiltration, solid-state diffusion of vanadium ions through the dense YSZ phase seems negligible compared to the other two at this temperature. This result supports findings in the literature[15] that vanadium has limited solubility in solid zirconia solid. The infiltration of vanadium through an interlamellar pore is demonstrated in Fig. 6(b). A secondary phase is observed in the gap between two parallel lamellar and EDS mapping confirmed it is rich in Y and V while displaying scarce Zr content as compared to the surrounding un-reacted lamella.

3.5. Effect of heat-treatment on pore connectivity and infiltration

Heat-treatment of plasma-sprayed coatings will tend to change the morphology of the interlamellar pores and intralamellar cracks. As these changes could influence the infiltration path of the molten vanadium oxide, hot corrosion tests at 800 °C for 90 min were performed on coatings previously heat-treated at 1000 °C and 1200 °C for 50 h. As shown by Erk et al.[23] heat-treatments at 1000 °C would activate only surface diffusion mass-transport mechanisms, and thus be non-densifying, while heat-treatments at 1200 °C would involve volume mass-transport mechanisms. Thus, coatings heat-treated at 1200 °C should densify. This reaction temperature and time were chosen as they represent a regime with sufficient infiltration of the molten vanadia to study the effects of the heat-treatments. As determined from the concentration profiles and microscopy observation, the penetration depth of the vanadium oxide into the as-sprayed and 1000 °C/50-h heat-treated coatings was 60 and

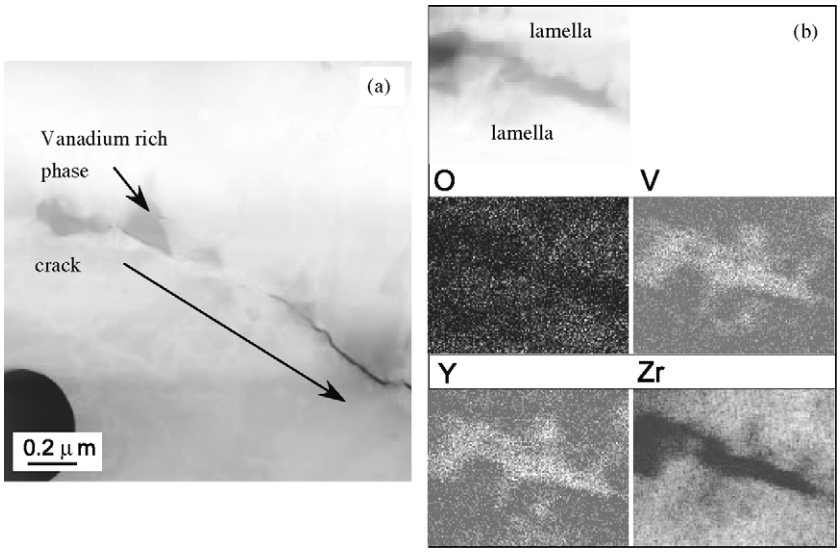

Fig. 6. STEM cross section images taken in MIRZ after the coating reacted with vanadium oxide at 750 °C for 180 min. (a) Vanadium-containing darker phase manifests along the crack. (b) EDS mapping of V, Y, Zr, and O along a filled interlamellar pore.

125 μm, respectively. The penetration depth of vanadium oxide in the as-sprayed coating and the 1200 °C/50-h heat-treated coating was ~60 μm and ~80 μm. The larger penetration depth of the coating heat-treated for 1000 °C/50 h versus the coating heat-treated for 1200 °C/50 h is an indication of enhanced permeability after the heat-treatment at 1000 °C.

4. Discussion

4.1. PRZ formation

The formation of the PRZ is governed primarily by the dissolution and reaction of the V_2O_5 with the surface layer of the YSZ coating. Dissolution of the YSZ coating occurs very quickly as Zr and Y were both detected using EDS in a partially reacted layer located on the surface of the coating after only 30 min at 750 °C (see Fig. 2). *In situ* XRD revealed that a ZrV_2O_7 phase, the reaction product between V_2O_5 and ZrO_2 at reaction temperatures of 700° and 750 °C, emerged at the beginning of the heat-treatments.[18] This indicates that the reaction products form very soon after dissolution. As shown in Fig. 3, increasing the reaction time increases the PRZ thickness, presumably due to the increased time for dissolving the coating.

The observed increase in PRZ thickness with increased reaction temperature (see Fig. 5) is attributed to the larger extent of dissolution by the V_2O_5. Increased solubility of zirconia in V_2O_5 as temperature increases is consistent with the ZrO_2–V_2O_5 binary phase diagram.[24] Therefore, the same amount of V_2O_5 has the capacity to dissolve a larger volume of the YSZ coating, and thus form a thicker PRZ, as reaction temperature increases. Likewise, increasing the amount of V_2O_5 added to the surface, while keeping reaction temperature constant, would also increase the thickness of the PRZ due to the increased amount of corrosive species available to dissolve the coating.

4.2. MIRZ formation

The MIRZ forms due to infiltration of the melted V_2O_5 via the pores and cracks common to plasma-sprayed coatings. Infiltration behavior has been modeled by Washburn[25] by considering capillary flow in cylindrical pores. The time, t, as a function of penetration depth, h, is given by:

$$t = \frac{2\eta}{\gamma \cos\theta} \frac{h^2}{R} \quad (1)$$

where η is the viscosity of the infiltrating liquid, γ is the surface tension of the liquid, θ is the equilibrium contact angle, and R is the radius of cylindrical pores.

While the wetting angle is not precisely known, $\cos\theta$ is taken as 1 as at all temperatures investigated currently as the liquid V_2O_5 spontaneously wets and infiltrates the YSZ. R is taken as 0.1 μm, which approximates the size of the smallest dimension of the fine porosity or cracks often found in these coatings. Using a γ value of 79 mN/m[26] and η value of 0.41 Pa s[27] for V_2O_5 melt at 750 °C, the calculated time using Eq. (1) to infiltrate through the thickness of a 300 μm coating is ~3 s. Analysis of Fig. 2 revealed a MIRZ thickness of 5 μm after 30 min at 750 °C. Clearly, the model and the experimental results do not agree. The major factors accounting for the difference between the experimental and modeled infiltration times regards the shape and size of the pores and/or cracks as the Washburn model assumption of a cylindrical pore geometry does not reflect the tortuosity of the pore network and non-uniform size of pores and cracks in the coating. Nor does the Washburn model account for changes in the pore morphology due to the dissolution of the YSZ by the molten V_2O_5 and/or the constriction of the pore by reaction products. Changes to the pore or crack structure are considered below.

The dissolution process should act to widen the pores and cracks (i.e. increase the R value), which according to the Wash-

burn equation, should increase the depth of infiltration. There is an increased amount of dissolution of the YSZ by the V_2O_5 as the reaction temperature is increased, as evidenced by the increase in PRZ thickness shown in Fig. 5. Enhanced infiltration due to widening of the pores and cracks is possibly occurring in the current data set, with MIRZ thicknesses of ~50, ~80, and ~130 μm observed after infiltration times of greater than 90 min at 750 °C, 800 °C, and 1000 °C, respectively. It is also possible to attribute the increase in infiltration depth with increasing temperature to the reduction in V_2O_5 viscosity. This is noted to decrease from 0.41 Pa s at 750 °C to 0.1 Pa s at 1000 °C,[27] which according to the Washburn equation should increase infiltration depth. While the decrease in viscosity over the noted temperature range is not dramatic, and therefore may have a limited effect on infiltration depth, further studies would be needed to delineate the contribution of dissolution and viscosity reduction on infiltration depth.

Further complicating the infiltration analysis is the formation of the reaction products. The t'-ZrO_2 + V_2O_5 transformation to m-ZrO_2 + YVO_4 results in a molar volume increase of 8–9%. These reaction products could act to block the further infiltration of the molten liquid. For reactions occurring from 70 to 420 min at 750 °C the MIRZ thickness was relatively constant at ~50 μm as a function of time. Similarly, reactions occurring at 800 °C demonstrated a constant affected depth of ~80 μm for times ranging from 30 to 150 min. The insensitivity of MIRZ thickness with time at constant reaction temperature suggests that unlimited infiltration does not occur into the coating, but rather, that reaction products may block the porous network of cracks and pores within ~70 min at 750 °C and ~30 min at 800 °C. The work presented here shows that the development of a model to describe infiltration phenomena with regard to material systems where dissolution of the host material, as well as the formation of reaction products, is greatly needed.

4.3. Interplay between dissolution, reaction, and infiltration rates

In general, the extent of the PRZ formation is governed by the dissolution and reaction rates of V_2O_5 with YSZ. If dissolution rates are low (i.e. low reaction temperatures and short times), then only minimal PRZ should be observed. For example, no PRZ was formed after 70 min at 750 °C, but a PRZ ~15–20 μm thick was formed after 180 min at the same temperature. If dissolution rates are high (i.e. high reaction temperatures and longer times) then a PRZ should be observed. For example, increasing reaction temperature for a constant reaction time of 90 min increased the PRZ thickness from ~10 μm at 900 °C to ~100 μm at 1200 °C.

The MIRZ thickness is likely influenced by the interplay between the infiltration, dissolution, and reaction rates of V_2O_5 with YSZ. Infiltration at 750° and 800 °C is dominated by the infiltration rate of the molten vanadia, but may be limited by the small dissolution rate of the pores which would limit the depth of penetration due to a smaller pore radius. Increased MIRZ thicknesses were noted for reactions between the YSZ coating and V_2O_5 from 900° and 1100 °C. Decreased viscosity of the vanadia along with increased dissolution rates of YSZ, which would open pores and cracks, would tend to increase infiltration depth. There is a limit to the effect of temperature, though, as the rate of reaction products formed also increases with temperature. The fact that no MIRZ was noted at 1200 °C is likely due to the rapid formation of reaction products that fill the pores and cracks, limiting infiltration rates. Thus, the V_2O_5 on the surface of the coating, which cannot infiltrate the coating, would be expected to react with the YSZ to form a PRZ. The interplay between dissolution, reaction, and infiltration is complex, and model experiments on cylindrical capillaries would help to delineate the effects of each.

4.4. Effect of pore microstructure on V_2O_5 melt infiltration

Heat-treatments representative of service conditions are known to affect the crack and pore morphology of plasma-sprayed coatings.[28] Using small angle neutron diffraction, Ilavasky et al. noted that intralamellar microcracks begin to close at 800 °C, and have completely healed by 1100 °C. Interlamellar pores begin to close at 1100 °C, and continue to close as temperature is increased. Thus, it would be expected that the effect of heat-treatments above 800 °C would tend to change infiltration due to changes in the morphology of the cracks, and heat-treatments above 1100 °C would change infiltration due to partial or complete closure of the pores. Thus, coating samples were heat-treated for 50 h at 1000 °C, to affect the crack morphology, and for 50 h at 1200 °C, to affect the pore morphology. Following the heat-treatments, 1 wt% V_2O_5 was applied to the surface and reacted for 90 min at 800 °C. This reaction temperature represents a regime with significant infiltration of molten vanadia into the coating expected.

As noted in the results section, the specimen heat-treated for 50-h at 1000 °C prior to reacting it with V_2O_5 at 800 °C for 90 min demonstrated a deeper penetration depth (125 μm) than for an as-sprayed coating reacted with V_2O_5 for 800 °C for 90 min (~60–80 μm). This result suggests enhanced connectivity of the pores and/or cracks is achieved after heat-treatment at 1000 °C that affords deeper penetration of the molten V_2O_5 into the coating. A possible explanation for this observed enhanced connectivity is a desintering process whereby the bridges that connect adjacent grains become detached. According to Sudre and Lange,[29] desintering or breaking up these bridges and replacing the grain boundaries with free surface is energetically more favorable if surface diffusion is the dominant mass transport mode and the distance between particle centers remains constant. Desintering in plasma-sprayed coatings at 1000 °C has been observed by Erk et al.[23] using AFM where large cracks opened up between columnar grains. In that same paper, Erk et al. [23] demonstrated that surface diffusion was the dominant mass transport mechanism at 1000 °C, a necessary condition for desintering. Thus, it is proposed that the 50-h heat-treatment at 1000 °C prior to application of the V_2O_5 opened up cracks perpendicular to the coating that allowed the molten species to infiltrate deep into the coating.

After a 50-h heat-treatment of the YSZ coating at 1200 °C, followed by reaction of the V_2O_5 at 800 °C for 90 min, the infiltration depth was similar to that of the as-sprayed coating. As

shown by Ilavasky et al.,[28] heat-treatments of plasma-sprayed YSZ at 1200 °C would be expected to close porosity, which in theory, should inhibit infiltration. However, the fact that the penetration depths were similar for both the as-sprayed and heat-treated coatings suggests that the decrease in porosity was not significant enough to limit the infiltration rate and/or dissolution rate of the YSZ coating by the molten V_2O_5.

5. Summary

Plasma-sprayed YSZ coatings used commonly as thermal barriers were coated with V_2O_5, a corrosive species found in less costly and less refined fuels, and reacted at temperatures ranging from 750° to 1200 °C and for times from 30 to 420 min. Two different morphologies were distinguished in cross-sectional views of V_2O_5-reacted plasma-sprayed YSZ coatings that correspond to a planar reacted zone and a melt infiltrated reaction zone. The morphology of the PRZ was fine-grained, and if it was observed for the reaction time and temperature investigated, began at the surface of the coating. The formation of the PRZ was a result of the dissolution of the top surface of the YSZ coating, followed by the formation of reaction products. Prolonged reaction times and higher temperature favors the formation of a thicker PRZ. The vanadium concentration, as measured using EDS, was equal to or greater than the yttrium concentration in the PRZ. Though not the focus of this paper, the final reaction products were a combination of ZrV_2O_7 and/or m-ZrO_2, and YVO_4, depending on the reaction temperature. The MIRZ appeared as a dense infiltrated region with the lamella structure still evident. The pores and cracks intrinsic to plasma-sprayed coatings were observed to be filled with reaction products via TEM/EDS investigations. Within the MIRZ, a fluctuating vanadium concentration was observed. If the probe was on a lamella then no vanadium was detected. If the probe was on a pore or crack adjacent to a lamella that had been filled by the molten V_2O_5, then vanadium was measured.

The thickness of the PRZ was determined by the dissolution and reaction rates of the V_2O_5 with the YSZ coating, with increased temperature and reaction times resulting in a thicker PRZ. The thickness of the MIRZ was the result of the interplay between the infiltration, dissolution, and reaction rates of the vanadium-containing liquid with the YSZ coating. Increased reaction temperatures increased the infiltration rate (by decreasing viscosity of the liquid) and dissolution rate (which tended to enlarge pores and cracks), but increased the formation rates of reaction products that can act to close the pores or cracks. Morphological parameters of the coating, such as pore size and connectivity, were found to influence the infiltration/reaction mechanisms. Prior heat-treatments of YSZ coatings at 1000 °C tended to increase the penetration depth due to a desintering process that opens up cracks on the surface of the coating.

References

1. Miller, R. A., Current status of thermal barrier coatings—an overview. *Surf. Coat. Technol.*, 1987, **30**, 1–11.
2. Goward, G., Progress in coatings for gas turbine airfoils. *Surf. Coat. Technol.*, 1998, **108–109**(1–3), 73–79.
3. Trembly, J. P., Gemmen, R. S. and Bayless, D. J., The effect of IGFC warm gas cleanup system conditions on the gas–solid partitioning and form of trace species in coal syngas and their interactions with SOFC anodes. *J. Power Sources*, 2007, **163**(2), 986–996.
4. Borom, M. P., Johnson, C. A. and Peluso, L. A., Role of environmental deposits and operating surface temperature in spallation of air plasma sprayed thermal barrier coatings. *Surf. Coat. Technol.*, 1996, **86–87**, 116–126.
5. Gurrappa, I., Thermal barrier coatings for hot corrosion resistance of CM 247 LC superalloy. *J. Mater. Sci. Lett.*, 1998, **17**, 1267–1269.
6. Leyens, C., Wright, I. G. and Pint, B. A., Hot corrosion of nickel-base alloys by alkali-containing sulfate deposits. *Mater. Sci. Forum*, 2001, **369–372**, 571–578.
7. Marple, B. R., Voyer, J., Moreau, C. and Nagy, D. R., Corrosion of thermal barrier coating by vanadium and sulfur compounds. *Mater. High Temp.*, 2000, **17**(3), 397–412.
8. Jones, R. L., Some aspects of the hot corrosion of thermal barrier coatings. *J. Thermal Spray Technol.*, 1997, **6**(1), 77–84.
9. Hamilton, J. C. and Nagelberg, A. S., In situ spectroscopic study of yttria-stabilized zirconia attack by molten sodium vanadate. *J. Am. Ceram. Soc.*, 1984, **67**(10), 686–690.
10. Kramer, S., Yang, J. and Levi, C. G., Thermochemical interaction of thermal barrier coatings with molten CaO-MgO-Al_2O_3-SiO_2 (CMAS) deposit. *J. Am. Ceram. Soc.*, 2006, **89**(10), 3167–3175.
11. Mercer, C., Faulhaber, S., Evans, A. G. and Darolia, R., A delamination mechanism for thermal barrier coatings subject to calcium-magnesium-alumino-silicate (CMAS) infiltration. *Acta Mater.*, 2005, **53**, 1029–1039.
12. Yoshiba, M., Abe, K., Aranami, T. and Harada, Y., High-temperature oxidation and hot corrosion behavior of two kinds of thermal barrier coating systems for advanced gas turbines. *J. Thermal Spray Technol.*, 1996, **5**(3), 259–268.
13. McKee, D. W., Luthra, K. L., Siemers, P. and Palko, J. E., Resistance of thermal barrier ceramic coatings to hot salt corrosion. In *Proceeding of the 1st Conference on Advanced Materials for Alternative Fuel Capable Directly Fired Heat Engines, CONF-790749*, ed. J. W. Fairbands and J. Stringer, 1979, pp. 258–269.
14. Rocca, E., Steinmetz, P. and Moliere, M., Revisiting the inhibition of vanadium-induced hot corrosion in gas turbines. *Trans. ASME*, 2003, **125**, 664–668.
15. Susnitzky, D. W., Hertl, W. and Carter, C. B., Destabilization of zirconia thermal barriers in the presence of V_2O_5. *J. Am. Ceram. Soc.*, 1988, **71**(11), 992–1004.
16. Luthra, K. and Spacil, H., Impurity deposits in gas-turbines from fuels containing sodium and vanadium. *J. Electrochem. Soc.*, 1982, **129**(3), 649–656.
17. Hertl, W., Vanadia reaction with yttria stabilized zirconia. *J. Appl. Phys.*, 1988, **63**(11), 5514–5520.
18. Chen, Z., Speakman, S., Howe, J., Wang, H., Porter, W. and Trice, R., Investigation of reactions between vanadium oxide and plasma-sprayed yttria-stabilized zirconia coatings. *J. Eur. Ceram. Soc.*, 2009, **29**, 1403–1411.
19. Kulkarni, A., Wang, Z., Nakamura, T., Sampat, S., Goland, A., Herman, H. *et al.*, Comprehensive microstructural characterization and predictive property modeling of plasma-sprayed zirconia coatings. *Acta Mater.*, 2003, **51**, 2457–2475.
20. Deschaseaux, C., A Sintering Study of Plasma-Sprayed Yttria-Stabilized Zirconia Thermal Barrier Coatings Using Stand Alone Coating Test, Master's Thesis, School of Materials Engineering, Purdue University, 2002.
21. Park, S. Y., Kim, J. H., Kim, M. C., Song, H. S. and Park, C. G., Microscopic observation of degradation behavior in yttria and ceria stabilized zirconia thermal barrier coatings under hot corrosion. *Surf. Coat. Technol.*, 2005, **190**, 357–365.
22. ASTM C373-77, "Standard Test Method for water absorption bulk density, apparent porosity and apparent specific gravity of fired whiteware products," 1997.

23. Erk, K., Deschaseaux, C. and Trice, R., Grain-boundary grooving of plasma-sprayed yttria-stabilized zirconia thermal barrier coatings. *J. Am. Ceram. Soc.*, 2006, **89**(5), 1673–1678.
24. M. K. Reser, ed. Phase Diagrams for Ceramists—1969 Supplement, Fig. 2405, American Ceramic Society, Columbus, OH, 1969.
25. Washburn, E. W., Dynamics of capillary flow. *Phys. Rev.*, 1921, **17**(3), 273–283.
26. Ikemiya, N., Umemoto, J., Hara, S. and Ogino, K., Surface tensions and densities of molten Al_2O_3, Ti_2O_3, V_2O_5 and Nb_2O_5. *ISIJ Int.*, 1993, **33**(1), 156–165.
27. Chacon-Tribin, H., Loftus, J. and Satterfield, C., Viscosity of the vanadium pentoxide-potassium sulfate eutectic. *J. Chem. Eng. Data*, 1966, **11**(1), 44–45.
28. Ilavsky, J., Long, G. G., Allen, A. J. and Berndt, C. C., Evolution of the void structure in plasma-sprayed YSZ deposits during heating. *Mater. Sci. Eng. A*, 1999, **A272**, 215–221.
29. Sudre, O. and Lange, F. F., The effect of inclusions on densification: III the de-sintering phenomenon. *J. Am. Ceram. Soc.*, 1992, **75**(12), 3241–3251.